Proceeding of the IEEE
International Conference on Robotics and Biomimetics
Dali, China, December 2019

A study on rotate vector reducer performance degradation based on acoustic emission techniques

Haibo An[1], Wei Liang[1,*] *Senior Member, IEEE,* Xiaojian Ding[3] Yinlong Zhang[2,*], and Jindong Tan[4] *Member, IEEE*

***Abstract*— This paper presents a performance degradation analysis for rotate vector (RV) reducer using acoustic emission (AE) techniques. Unlike the AE signals from fixed gear reducer that are steady and have unchanged route, the AE signals from RV reducer have variant propagation paths and strengths. This work investigates the kinematics model using AE techniques to solve the inherent issues of RV reducer performance degradation analysis, such as signal variabilities and inappropriate thresholds. Firstly, the propagation path of AE signals within the crankshaft is developed. Secondly, the attenuation trend of AE signals is exponentially formulated based on the corresponding propagation curve. The proposed method has been evaluated on the developed RV reducer platform. AE signals were collected under various working conditions, i.e., four abrasion states with eight types of loads and five rotation speeds. The experimental analysis on typical parameters (e.g., signal energies) proves the effectiveness and accuracy of the developed method based on AE techniques.**

I. Introduction

Rotate vector (RV) reducer is an indispensable component in industrial robotics. System precision and efficiency largely depends on RV reducer performance. However, what inevitably happens is that robitic heavy-load and long-term operation will result in reducer overall performance degradations [1], such as typical abrasions and fractures. Thus, the evaluation on RV reducer degradation plays a critical role in maintaining the robots running stably and reliably in the long run [2]–[7]. To this end, this paper presents a performance degradation mechanism for RV reducer using acoustic emission techniques.

Different from fixed gear mechanical structure, RV reducer structure features in two-speed reduction mechanism, i.e., planetary gear & cycloid, shown in Fig. 1. Among the main components of RV reducer, crankshaft is the largest part being stressed, and also the part being severely worn. Unlike the signals produced from fixed gear, which are constant and mostly unchanged [8], [9], the abrasion signals from the crankshaft will be variant on intensity and phase over time, due to the fact that the propagation path of the signal changes over the rotation of cam disk [10]–[13].

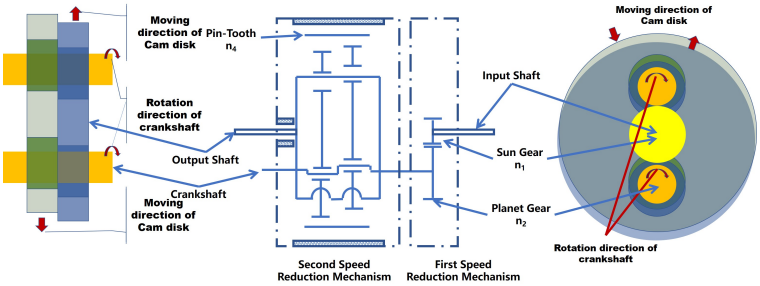

Fig. 1. Structure of RV reducer.

To obtain the propagation path of AE signal within RV reducer produced by crankshaft and to achieve the corresponding attenuation curve, we establish the propagation model of AE signal within the RV reducer. Specifically, the kinematics model of cam disk is developed to derive the propagation path of Acoustic Emission (AE) signals within the crankshaft. Afterwards, the attenuation trend of AE signals is exponentially formulated based on the corresponding propagation curve.

In this work, the reducer kinematic model is investigated and the geometry relationship between the crankshaft and cam disk inside the reducer is analyzed. Then the acoustic emission (AE) techniques are utilized to derive the propagation path. Finally, the attenuation model for the acoustic signals from the mechanical parts that are worn are derived.

The remaining parts of this paper are organized as follows. In Section II, the related works on RV reducer performance degradations are described. Section III introduces the theoretical model of the acoustic signal propagation within the RV reducer. Section IV describes the experimental platform and the degradation tests & analysis. Conclusions are drawn in Section V.

II. Relate Works

Many researchers have already focused on the fault mechanism analysis of gear reducer or cycloidal-pin gear speed reducer, such as Chu [14]. The authors presented a detailed analysis on planet gear reducer. Although that work has taken

1. Haibo An and Wei Liang (corresponding author) are with the State Key Laboratory of Robotics, Chinese Academy of Sciences, Shenyang 110016, China and with the Key Laboratory of Networked Control Systems, Shenyang Institute of Automation, Chinese Academy of Sciences, Shenyang, 110016, China and with Institutes for Robotics and Intelligent Manufacturing, Chinese Academy of Sciences, Shenyang 110016, China and with University of Chinese Academy of Sciences, Beijing, 100049, China. email:{anhaibo, weiliang}@sia.cn

2. Yinlong Zhang (corresponding author) is with Shenyang Institute of Automation, Guangzhou, Chinese Academy of Sciences, Guangzhou, 511548, China and with the Key Laboratory of Networked Control Systems, Shenyang Institute of Automation, Chinese Academy of Sciences, Shenyang, 110016, China and with Institutes for Robotics and Intelligent Manufacturing, Chinese Academy of Sciences, Shenyang 110016, China. email: zhangyinlong@sia.cn

3. Xiaojian Ding is with The Fifth Electronic Institute of MIIT, Guangzhou 510610, China. email: dingxiaojian0923@126.com

4. Jindong Tan is with the Department of Mechanical, Aerospace and Biomedical Engineering, University of Tennessee, Konxville, TN, 37996, USA. email: tan@utk.edu

978-1-7281-6321-5/19//$31.00 ©2019 IEEE

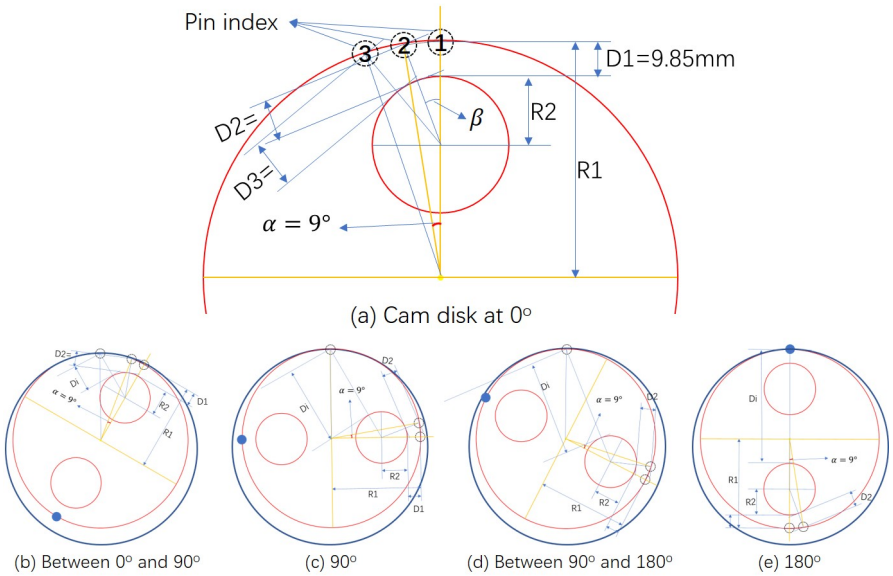

Fig. 2. AE signal propagation path within the RV reducer cam disk

vibration signals into acount, it only analyzed the fault tendency. Blagojevic et al. [15] took a comprehensive analysis on the influence of the friction on the cycloid reducer. Lei et al. [16], [17] have performed the overload fatigue tests on the bearing and dealt with the vibration signals based on theoretical analysis. Various researchers have begun to use AE signals to analyze the abrasion states of the reducer. For example, Yoon et al. [18] used acoustic signals to derive the states of the planetary gearbox; Kia [11] and Zhou [10] made a comparative study between the acoustic and vibration signals and proved that the acoustic emission is better on the condition monitoring than vibration signals. Li et al. [19] have made a detailed research to analyze the rotational machine health monitoring and fault detection using EMD-based acoustic emission feature quantification to fulfill the signal analysis in rotational machines.

The researches on RV reducer kinematics and internal structures have been well studied. For instance, Wang et al. [20] investigated the relationship between the stiffness of the RV reducer and the profile modification method of the cycloid-pin wheel. Zhang [21] made a detailed analysis on the formulation of the RV reducer. Likewise, Bo [22] conducted the research on the lubrication performance in different abrasion states. Also there were several researchers which tried to monitor the RV reducer conditions, such as [23] and [2]. However, there were few researches on RV reducer condition monitoring, since most research works only focused on analyzing the internal structure of RV reducer. And there are still further potentials for the study on RV reducer performance degradation mechanism.

III. Models

As the industrial robot transmission mechanical part, RV reducer is able to transform the power of servo motor with high speed and low torque to the corresponding reducer outputs with low speed and high torque. The RV reducer structure has two-stage speed reductions: planetary speed reduction and cycloidal pinwheel speed reduction, as shown in Fig. 1. For the first stage, the reduction ratio N_1 is given by

$$N_1 = n_2/n_1 \tag{1}$$

where n_1 denotes the sun gear tooth number and n_2 represents the planetary gear tooth number. For the second stage, the reduction ratio N_2 is given by

$$N_2 = n_4/(n_4 - n_3) \tag{2}$$

where n_3 means the pin wheel of cam disk; n_4 is the number of gear pins in the shell.

Because of the fact that the difference between the number of cam disk wheel pins and the number of gear pins in the shell is $n_4 - n_3$, both of the output shaft and cam disk rotate one circle; and the crankshaft rotates N_2 circles. Consequently, the period of reunion between the toothed disk and the fixed point of the shell is n_3, i.e., the crankshaft rotates n_4 circles, which could be reflected by the AE signal.

AE is the phenomenon of radiation of elastic waves caused by irreversible changes in material internal structure. The signal intensity is exponentially decreased with the propagation distance. The AE propagation strength is given by

$$p(x) = p_0 e^{-\zeta x} \tag{3}$$

where x is the propagation distance; ζ is the decay index (which is determined by the propagation materials); p_0 is the signal intensity from the emission source. The structure of RV reducer is complicated and the reducer has numerous signal sources. This paper holds the assumption that the medium upon which the signal propagates is uniform in an equidistant fashion. Because the relative position between the pin gear and the shell is fixed, and the relative position

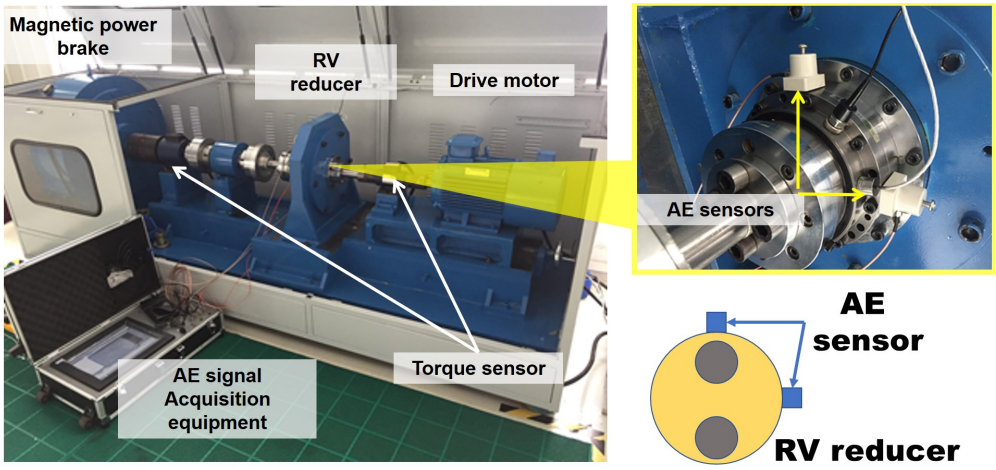

Fig. 3. RV reducer platform

between the cam disk and crankshaft is fixed, we are able to calculate the propagation path of the AE signals from the crankshaft to cam disk and via the pinwheel to the shell. As a result, the intensity of the AE signal could be derived using Eq. 3.

As shown in Fig. 2, the radius of the cam disk is R_1; the radius of the crankshaft hole is R_2; α is the angle between the two adjacent pin wheel and the center of cam disk; D_1 is the distance between No. 1 pin wheel and the crankshaft hole; D_i is the i_{th} distance between the i_{th} pin wheel with the crankshaft hole; β_i is the angle of the i_{th} pin wheel and the first pin wheel with the center of the crankshaft hole. From the geometrical derivation, the propagation distance is as follows:

$$\begin{aligned} D_i &= \sqrt{R_1^2 + L^2 - 2R_1 \cdot L \cdot \cos(\alpha \cdot i)} - R_2 \\ L &= R_1 - R_2 - D_1 \end{aligned} \tag{4}$$

The distance between the sensor and the crankshaft hole in different rotation angles of the cam disk could also be calculated, which are shown in Fig. 2(b $\sim$ e). Fig. 2(b) is the status that the cam disk rotates between 0° and 90°; Fig. 2(c) is the status that the cam disk at 90°; Fig. 2(d) is the status that the cam disk at the angle range between 90° and 180° and Fig. 2(e) is the status that the rotation at 180°. Suppose that the AE signal produced from the contact surface between the crankshaft and cam disk is uniformly distributed, which also means the crankshaft and cam disk is uniformly contacted. On the basis of this assumption, we are able to compute the distance between the cam disk inner hole and the outside shell, which in our case is 9.85 mm. And we take this distance as unit one. Based on Eq. 4, the signal relative strengths are shown in Table 1.

TABLE I
AE SIGNAL PROPAGATION STRENGTH OF CAM DISK

No.	Angle	distance(mm)	normalization (x)	$1/e^x$
0	0	9.85	1.0	1.0
1	9	10.7914462	1.0955783	0.9088473
2	18	13.4262464	1.3630707	0.6955374
3	27	17.3228041	1.7586603	0.4682936
4	36	22.0352050	2.2370813	0.2902303
5	45	27.2130098	2.7627421	0.1757395
6	54	32.6065967	3.3103144	0.0992302
7	63	38.0403975	3.8619693	0.0571562
8	72	43.3876424	4.4048368	0.0332123
9	81	48.5531045	4.9292492	0.0196585
10	90	53.4623852	5.4276533	0.0119425

IV. Experiments and Results

In the experiment, the developed platform for RV reducer test mainly consists of AC speed motor, speed & torque sensors and magnetic powder brake, as can be seen in Fig. 3. The AC speed motor provides the input speed (ranges between 0 and 2000 r/min). The input torque sensor measures the torque between 0 and 50 N · m, with the measurement error less than 0.5%; the output torque sensor measures the output torque between 0 and 5000 N·m, with the measurement error less than 0.5%. The maximum torque from magnetic powder could reach up to 5000 N·m, which could meet the requirements of the reducer tests.

In our tests, the data acquisition equipment (DAE) are the AE sensors, which are magnetically attached to the surface of the RV shell and the angle between these two sensors is 90°, shown in Fig. 3. DAE could sample the two-channel AE signals synchronously with the sample frequency as high as 10 M/s which could cover the main frequency of AE signal ranges (i.e., 20KHz $\sim$ 300KHz) based on Shannon sampling theorem.

To fulfill the accelerated degradation, the higher stress was enforced on the RV reducer output. In the tests, Arrhenius model is adopted to describe the degrees of overload degradations.

In the accelerated degradation tests, the output rotation speed was chosen as 15 r/min and the load was set as 1000 N·m, which was 2.5 times higher than the specified load that was 412 N · m. The overload test lasted about two hours, which could approximate the performance of the RV reducer

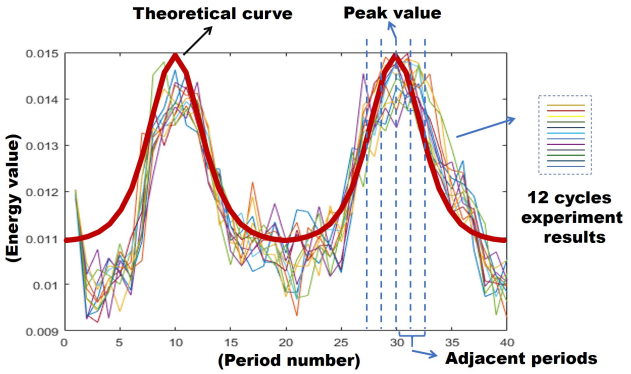

Fig. 4. Energy curves of 39 periods

which operates in the normal working conditions for several months. After the degradation test, the reducer accuracy decreased by 10 arc/sec. Before the degradation test, the AE signals were collected under various combinations of speeds and loads. The rotation speed started at 4 r/min and followed by 6 r/min, 8 r/min, 10 r/min, 12 r/min, 14 r/min and 15 r/min. The output torque was tuned from 50 N· m to 400 N· m by 50 N·m at each time.

The AE sensors, which are vertically fixed on the reducer shelf, collected the AE signals and transmitted the data to the computer through the two-channel devices (shown in Fig. 3). The comparisons on the phases of the peak waves prove that the AE signals are from the inner cam disk and crankshaft from the reducer. As shown in Fig. 5, there are 39 waves (separated by red dashed lines), which are uniformly spanned among the whole sampling process. Each wave features in two sub-waves. The right part is the wave peak that has been partially enlarged. The red solid line on top of each wave peak represents the theoretical signal magnitude. It can be seen that there are several derivations between the peak wave and the corresponding analytical derivations. Part of the reason for this derivation lies in the distance bias between the AE sensor position and the crankshaft center.

On the basis of the above analysis, the energy indexes within the 39 waves are calculated. The corresponding energy curves within the 12 consecutive cycles are shown in Fig. 4. As can be seen, there are 12 continuous circles of AE signals displayed by thinner curve and the red thick line deduced from the theoretical model in Eq. 3 and Eq. 4. In this case, the output speed is 14 r/min, and the torque is 400 N · m. It can be seen that the signal energy curve approximates the theoretical parts. As can be seen in Table 1, the signal strength attenuates below half of the peak value after index No. 4, so we only analyze the AE signal above 50% attenuation within 2 or 3 adjacent periods. Through this way, the useful signals with smaller attenuation can be acquired and the computational efficiency can be improved by 70 % to 80 %.

V. Conclusion

In this ppaer, an effective method that uses AE techniques to evaluate the RV reducer degradation has been presented. The RV reducer kinematics model and the AE signal propagation inside have been thoroughly investigated. The corresponding potential features in time domain for reducer abrasions have been analyzed. Meanwhile, the processing speed has been increased since the signal analysis has been focused on the parts that are rich in abrasion information. Through this way, the computational time has been shortened by 20% to 30%, which could significantly accelerate the abrasion evaluation process for industrial robotics. The experimental results and analysis prove the effectiveness and accuracy of the proposed method.

VI. Acknowledgement

The authors would like to thank the editor and reviewers for their valuable suggestions and comments. This work has been supported in part by the National Key Research and Development Program of China (2017YFE0101200 and 2017YFE0123000),the Key Research and Development Program of Guangdong Province (2019B090916001), National Natural Science Foundation of China (71661147005 and 61903357), International Partnership Program of Chinese Academy of Sciences (173321KYSB20180020), Liaoning Provincial Natural Science Foundation of China (2019-YQ-09), and Pearl River Nova Program of Guangzhou (201605131121390).

References

[1] Y. Lei, J. Lin, Z. He, and M. J. Zuo, "A review on empirical mode decomposition in fault diagnosis of rotating machinery," *Mechanical systems and signal processing*, vol. 35, no. 1-2, pp. 108–126, 2013.

[2] H. An, W. Liang, Y. Zhang, Y. Li, S. Lu, and J. Tan, "Retrogressive analysis of industrial robot rotate vector reducer using acoustic emission techniques," in *2018 IEEE 8th Annual International Conference on CYBER Technology in Automation, Control, and Intelligent Systems (CYBER)*. IEEE, 2018, pp. 366–372.

[3] A. Hase, H. Mishina, and M. Wada, "Correlation between features of acoustic emission signals and mechanical wear mechanisms," *Wear*, vol. 292, pp. 144–150, 2012.

[4] G.-A. Capolino, J. A. Antonino-Daviu, and M. Riera-Guasp, "Modern diagnostics techniques for electrical machines, power electronics, and drives," *IEEE Transactions on Industrial Electronics*, vol. 62, no. 3, pp. 1738–1745, 2015.

[5] S. H. Kia, H. Henao, and G.-A. Capolino, "Gear tooth surface damage fault detection using induction machine stator current space vector analysis," *IEEE Transactions on industrial Electronics*, vol. 62, no. 3, pp. 1866–1878, 2014.

[6] H. An, W. Liang, Y. Zhang, Y. Li, Y. Liang, and J. Tan, "Rotate vector reducer crankshaft fault diagnosis using acoustic emission techniques," in *2017 5th International Conference on Enterprise Systems (ES)*. IEEE, 2017, pp. 294–298.

[7] Z. Yi and A. H. Etemadi, "Line-to-line fault detection for photovoltaic arrays based on multiresolution signal decomposition and two-stage support vector machine," *IEEE Transactions on Industrial Electronics*, vol. 64, no. 11, pp. 8546–8556, 2017.

[8] M. D. Prieto and D. Z. Millán, "Chromatic monitoring of gear mechanical degradation based on acoustic emission," *IEEE Transactions on Industrial Electronics*, vol. 64, no. 11, pp. 8707–8717, 2017.

[9] S. Li, "Design and strength analysis methods of the trochoidal gear reducers," *Mechanism and Machine Theory*, vol. 81, pp. 140–154, 2014.

[10] L. Zhou, F. Duan, D. Mba, and E. Faris, "A comparative study of helicopter planetary bearing diagnosis with vibration and acoustic emission data," in *2017 IEEE International Conference on Prognostics and Health Management (ICPHM)*. IEEE, 2017, pp. 246–251.

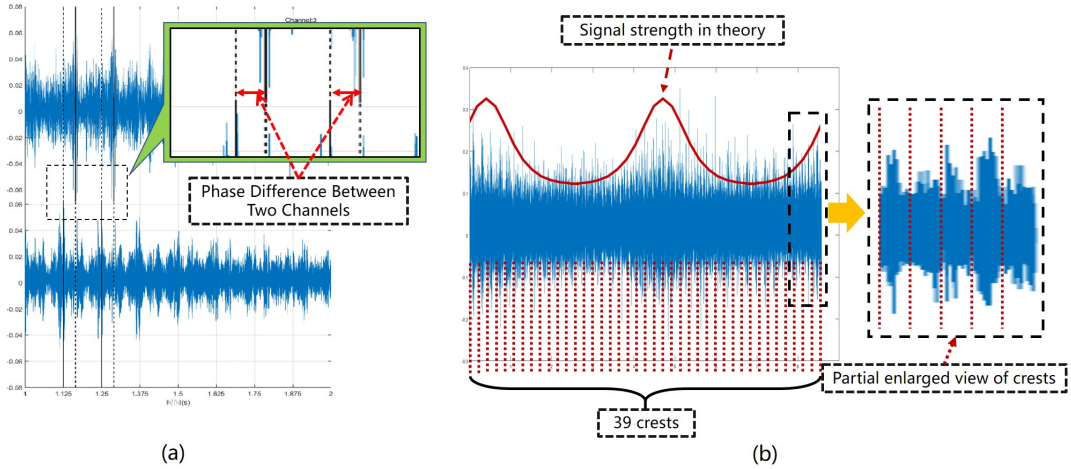

Fig. 5. AE signal analysis in time domain

[11] S. H. Kia, H. Henao, and G.-A. Capolino, "A comparative study of acoustic, vibration and stator current signatures for gear tooth fault diagnosis," in *2012 XXth International Conference on Electrical Machines*. IEEE, 2012, pp. 1514–1519.

[12] X. Xia, Y. Xiao, and W. Liang, "Absi: An adaptive binary splitting algorithm for malicious meter inspection in smart grid," *IEEE Transactions on Information Forensics and Security*, vol. 14, no. 2, pp. 445–458, 2018.

[13] A. Steinwolf, "Vibration testing of vehicle components by random excitations with increased kurtosis," *International Journal of Vehicle Noise and Vibration*, vol. 11, no. 1, pp. 39–66, 2015.

[14] Y. Zhang, W. Lu, and F. Chu, "Planet gear fault localization for wind turbine gearbox using acoustic emission signals," *Renewable Energy*, vol. 109, pp. 449–460, 2017.

[15] M. Blagojevic, M. Kocic, N. Marjanovic, B. Stojanovic, Z. Dordevic, L. Ivanovic, and V. Marjanovic, "Influence of the friction on the cycloidal speed reducer efficiency," *Journal of the Balkan Tribological Association*, vol. 18, no. 2, pp. 217–227, 2012.

[16] N. Li, Y. Lei, L. Guo, T. Yan, and J. Lin, "Remaining useful life prediction based on a general expression of stochastic process models," *IEEE Transactions on Industrial Electronics*, vol. 64, no. 7, pp. 5709–5718, 2017.

[17] Y. Lei, F. Jia, J. Lin, S. Xing, and S. X. Ding, "An intelligent fault diagnosis method using unsupervised feature learning towards mechanical big data," *IEEE Transactions on Industrial Electronics*, vol. 63, no. 5, pp. 3137–3147, 2016.

[18] J. Yoon and D. He, "Planetary gearbox fault diagnostic method using acoustic emission sensors," *IET Science, Measurement & Technology*, vol. 9, no. 8, pp. 936–944, 2015.

[19] R. Li and D. He, "Rotational machine health monitoring and fault detection using emd-based acoustic emission feature quantification," *IEEE Transactions on Instrumentation and Measurement*, vol. 61, no. 4, pp. 990–1001, 2012.

[20] J. Wang, J. Gu, and Y. Yan, "Study on the relationship between the stiffness of rv reducer and the profile modification method of cycloid-pin wheel," in *International conference on intelligent robotics and applications*. Springer, 2016, pp. 721–735.

[21] Y. Zhang, J. Xiao, and W. He, "Dynamical formulation and analysis of rv reducer," in *2009 International Conference on Engineering Computation*. IEEE, 2009, pp. 201–204.

[22] W. Bo, W. Jiaxu, Z. Guangwu, Y. Rongsong, Z. Hongjun, and H. Tao, "Mixed lubrication analysis of modified cycloidal gear used in the rv reducer," *Proceedings of the Institution of Mechanical Engineers, Part J: Journal of Engineering Tribology*, vol. 230, no. 2, pp. 121–134, 2016.

[23] J. Ge, B. Lu, Y. Wang, and X. Jiang, "Research on accelerated degradation test of rv reducer," *International Journal of control and automation*, vol. 10, no. 1, pp. 209–216, 2017.